

# Room-temperature continuous-wave operation of long wavelength ( $\lambda = 9.5 \mu\text{m}$ ) MOVPE-grown quantum cascade lasers

C. Pflügl, L. Diehl, A. Tsekoun, R. Go, C.K.N. Patel, X. Wang, J. Fan, T. Tanbun-Ek and F. Capasso

High-power continuous-wave operation of long wavelength quantum cascade lasers grown by metal organic vapour phase epitaxy is reported. The lasers have been processed as buried heterostructures with thick gold-plated contacts. The devices emit at a wavelength of  $9.5 \mu\text{m}$  with output powers of several hundreds of milliwatts at room temperature.

**Introduction:** Many spectroscopic applications in the mid-infrared wavelength range demand high performance coherent light sources operating in continuous wave (CW) above room temperature. Especially the atmospheric transmission windows (3–5 and 8–13  $\mu\text{m}$ ) are very important for remote sensing of pollutant and toxic gases and for free-space optical communications. Both spectral regions can be covered by quantum cascade lasers (QCLs). Continuous-wave operation above room temperature was demonstrated at wavelengths around 10  $\mu\text{m}$  [1, 2] using molecular beam epitaxy (MBE)-grown material. At longer wavelengths the performance is limited mainly by optical losses due to free-carrier absorption. Extension of QCL emission to longer wavelengths requires the growth of samples with thinner barriers, placing higher demands on the control of interface abruptness during the growth process. This is an important issue especially for QCLs grown by metal organic vapour phase epitaxy (MOVPE), which is a widely established platform for the high-volume production of reliable optoelectronic devices. Especially at longer wavelengths, MOVPE growth has the additional advantage that the thick InP cladding layers can be deposited at a very fast growth rate in the same growth run as the active region. It has already been demonstrated that MOVPE-grown QCLs show performance comparable to the best MBE-grown devices up to 8.4  $\mu\text{m}$  [3–5]. Although pulsed operation above room temperature was demonstrated at 10.3  $\mu\text{m}$  [6] and 11.3  $\mu\text{m}$  [7] the question arises whether the growth and layer interface qualities of MOVPE QCL structures are comparable to those of MBE grown structures.

In this Letter we report the performance of MOVPE-grown epi-down mounted QCLs emitting at  $9.5 \mu\text{m}$  in CW at room temperature (RT). The maximum collected output power from a 13  $\mu\text{m}$ -wide and 5 mm-long device was 180 mW per facet at 295 K with a wall-plug efficiency of 1.9% (including the output of both facets).

**Fabrication and measurement techniques:** The structure was grown by MOVPE with the following layer sequence. Thirty-five periods of a 2-Phonon design [8] active region are used as the active core and sandwiched between two 0.5  $\mu\text{m}$ -thick *n*-doped ( $1.5 \times 10^{16} \text{ cm}^{-3}$ )  $\text{In}_{0.53}\text{Ga}_{0.47}\text{As}$  layers. The upper cladding layers consist of 3.5  $\mu\text{m}$ -thick *n*-doped ( $5 \times 10^{16} \text{ cm}^{-3}$ ) InP, followed by a 0.5  $\mu\text{m}$ -thick *n*-doped ( $2.5 \times 10^{18} \text{ cm}^{-3}$ ) InP cap layer. The lower cladding consists of a 3.5  $\mu\text{m}$ -thick *n*-doped ( $5 \times 10^{16} \text{ cm}^{-3}$ ) InP layer grown on a highly doped substrate ( $3 \times 10^{18} \text{ cm}^{-3}$ ). The average doping in the active region is  $8.1 \times 10^{15} \text{ cm}^{-3}$ . The waveguide loss is calculated to be  $\alpha_w = 6 \text{ cm}^{-1}$  and the confinement factor  $\Gamma$  is 0.5.

Buried heterostructure lasers were processed using conventional fabrication techniques [9]. Ridges with a width of either 9 or 13  $\mu\text{m}$  were fabricated by wet etching. Fe-doped InP was then regrown to planarise the structure, helping to decouple laterally the optical mode from the lossy metal contacts and to lower the thermal resistance of the device while minimising leakage currents. Electrical contacts are provided by Ti/Au metallisation evaporated directly onto the *n*+InGaAs capping layer and the Fe:InP surrounding the laser ridge. An additional 5  $\mu\text{m}$ -thick gold layer was subsequently electroplated on the top contact to further improve heat dissipation. The devices were cleaved and the cleaved facets were left uncoated. For pulsed measurements, the devices were mounted ridge side up onto copper blocks and wire bonded. For CW measurements, the devices were mounted epi-side down. The 3 mm-long cavity devices were mounted epi-down on AlN submounts with hard AuSn solder [10]. An integrated thermistor was provided on the submount, located approximately 1 mm away from the laser. The chip-on-carrier assemblies were further soldered to Cu

heat spreaders, and mounted onto thermoelectric coolers. The longer cavity devices were mounted epi-down on copper blocks with indium solder using traditional methods.

The 3 mm-long devices were measured under active temperature control, where the thermistor signal was used as feedback to a thermoelectric cooler in order to maintain the chip-on-carrier assembly at constant temperature despite the increase in laser drive current. The longer devices were temperature controlled in a passive manner by means of a constant temperature, water-cooled heatsink to which the device mounts were attached. Optical power measurements were performed with a calibrated large area thermopile detector positioned as close to the output facet of the devices as possible. No correction was introduced for collection efficiency.

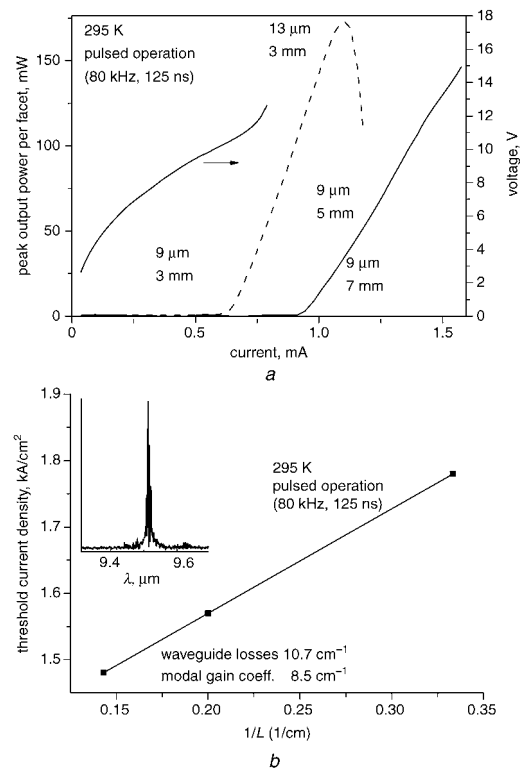


**Fig. 1** Output power against current characteristics for devices with different ridge widths and lengths, and measured pulsed threshold current density against reciprocal cavity length at 295 K

**a** Output power against current characteristics for devices with different ridge widths and lengths (solid line: 9  $\mu\text{m}$ -wide devices; dashed line: 3 mm-long and 13  $\mu\text{m}$ -wide device). For 3 mm-long and 9  $\mu\text{m}$ -wide device V-I curve also shown  
**b** Measured pulsed threshold current density against reciprocal cavity length at 295 K. Solid line is result of linear least squares fit  
 Inset: Spectrum of this device at room temperature (pulsed operation)

**Characterisation:** Fig. 1a shows the pulsed (80 kHz, 125 ns) VI-, LI-characteristics of 9  $\mu\text{m}$ -wide devices and a 3 mm-long device at room temperature (295 K). Additionally, the LI-characteristics of devices with different dimensions are shown. The emission wavelength at RT is 9.5  $\mu\text{m}$  (see inset of Fig. 1b). The slope efficiency decreases from 380 mW/A for a 3 mm-long device to 242 mW/A (272 mW/A) for a 7 mm (5 mm)-long device owing to decreasing mirror losses. Also, the decreasing threshold with increasing length is a manifestation of the reduced mirror losses. From this dependence, we can deduce the waveguide losses and the modal gain coefficient. Fig. 1b shows the threshold current density against the inverse of the length of the devices. A linear fit gives a modal gain coefficient of 8.5 cm/kA and waveguide losses of 10.7 cm<sup>-1</sup>. The measured losses are higher than those obtained with a two-dimensional simulation. The simulation, however, only includes losses due to free-carrier absorption and neglects optical losses caused by intersubband absorption in the injector and scattering losses. One scattering mechanism is sidewall scattering along the laser ridge. It depends on the width of the devices as the optical mode overlap with the sidewall increases with decreasing ridge width. In our case the threshold current density measured in pulsed operation is reduced from 1.78 kA/cm<sup>2</sup> for a 9  $\mu\text{m}$ -wide and

3 mm-long device to  $1.65 \text{ kA/cm}^2$  for a  $13 \mu\text{m}$ -wide device with the same length. This corresponds to a decrease in waveguide losses of about  $1 \text{ cm}^{-1}$ . Although narrower ridges have slightly higher losses, buried heterostructures have the advantage that the refractive index change between the active area and the overgrown material is very small, which reduces significantly the losses due to sidewall scattering compared to conventional ridge waveguide designs with insulator/metal sidewalls. Further improvements of our devices are expected by decreasing the doping in the waveguide layers as this significantly decreases the free-carrier absorption losses at longer wavelength. Recent work on long wavelength QCLs has shown that the losses due to free-carrier absorption can further be reduced without significantly increasing the series resistance [2].

The devices were also tested in CW operation (Fig. 2). A 3 mm-long and  $9 \mu\text{m}$ -wide device had a threshold current density of  $1.9 \text{ kA/cm}^2$  and a slope efficiency of  $245 \text{ mW/A}$ . The maximum output power for this device per facet was  $48 \text{ mW}$  at a current density of  $2.6 \text{ kA/cm}^2$ . We further tested a 5 mm-long and  $13 \mu\text{m}$ -wide device in CW operation. The threshold current density for this device at RT was as low as  $1.54 \text{ kA/cm}^2$ . The output power per facet for this device is  $180 \text{ mW}$  at RT and  $220 \text{ mW}$  at  $14^\circ\text{C}$ . This corresponds to a wall-plug efficiency of 1.9% (2.3%) if one includes the output for both facets  $360 \text{ mW}$  ( $440 \text{ mW}$ ) at RT ( $14^\circ\text{C}$ ).

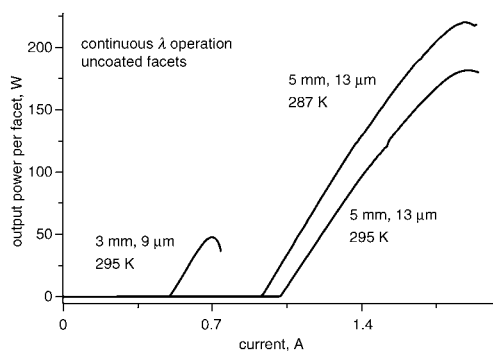


**Fig. 2** *L-I characteristics of devices with different length and width operated in continuous wave (facets of devices left uncoated)*

**Conclusion:** We have demonstrated high performance QCLs grown by MOVPE operating at  $9.5 \mu\text{m}$ . The performance of these devices is comparable to the best devices grown by MBE. Further improvements in bandstructure engineering and waveguide design, especially by further decreasing the doping in the waveguide layers, should make the high-power CW operation of MOVPE-grown QCLs feasible in the whole atmospheric window range (up to  $13 \mu\text{m}$ ).

**Acknowledgement:** The authors acknowledge financial support from NIST's Advanced Technology Program under contract 70NANB3H3026.

© The Institution of Engineering and Technology 2007  
25 July 2007

*Electronics Letters* online no: 20072162

doi: 10.1049/el:20072162

C. Pflügl, L. Diehl and F. Capasso (*Harvard School of Engineering and Applied Sciences, Harvard University, Cambridge, MA 02138, USA*)

E-mail: pflugl@seas.harvard.edu

A. Tsekoun, R. Go and C.K.N. Patel (*Pranalytica, Inc., 1101 Colorado Avenue, Santa Monica, CA 90401, USA*)

X. Wang, J. Fan and T. Tanbun-Ek (*Adtech Optics, Inc., 18007 Cortney Court, City of Industry, CA, 91748, USA*)

C.K.N. Patel: Also with the Department of Physics & Astronomy, University of California, Los Angeles, CA, 90095, USA

## References

- 1 Yu, J.S., Slivken, S., Evans, A., Darvish, S.R., Nguyen, J., and Razeghi, M.: 'High-power  $\lambda=9.5 \mu\text{m}$  quantum-cascade lasers operating above room temperature in continuous-wave mode', *Appl. Phys. Lett.*, 2006, **88**, p. 091113
- 2 Slivken, S., Evans, A., Zhang, W., and Razeghi, M.: 'High-power, continuous-operation intersubband laser for wavelengths greater than  $10 \mu\text{m}$ ', *Appl. Phys. Lett.*, 2007, **90**, p. 151115
- 3 Troccoli, M., Corzine, S., Bour, D., Zhu, J., Assayag, O., Diehl, L., Lee, G., Höfler, G., and Capasso, F.: 'Room temperature continuous-wave operation of quantum-cascade lasers grown by metal organic vapour phase epitaxy', *Electron. Lett.*, 2005, **41**, p. 1059
- 4 Diehl, L., Bour, D., Corzine, S., Zhu, J., Höfler, G., Lončar, M., Troccoli, F., and Capasso, F.: 'High-power quantum cascade lasers grown by low-pressure metal organic vapor-phase epitaxy operating in continuous wave above  $400 \text{ K}$ ', *Appl. Phys. Lett.*, 2006, **88**, p. 201115
- 5 Diehl, L., Bour, D., Corzine, S., Zhu, J., Höfler, G., Lončar, M., Troccoli, F., and Capasso, F.: 'High-temperature continuous wave operation of strain-balanced quantum cascade lasers grown by metal organic vapor-phase epitaxy', *Appl. Phys. Lett.*, 2006, **89**, p. 081101
- 6 Green, R.P., Wilson, L.R., Zibik, E.A., Revin, D.G., Cockburn, J.W., Pflügl, C., Schrenk, W., Strasser, G., Krysa, A.B., Roberts, J.S., Tey, A.G., and Cullis, A.G.: 'High-performance distributed feedback quantum cascade lasers grown by metalorganic vapor phase epitaxy', *Appl. Phys. Lett.*, 2004, **85**, p. 5529
- 7 Moreau, V., Krysa, A.B., Bahriz, M., Wilson, L.R., Colombelli, R., Revin, D.G., Julien, F., Cockburn, J.W., and Roberts, J.S.: 'Pulsed operation of long-wavelength ( $\lambda = 11.3 \mu\text{m}$ ) MOVPE-grown quantum cascade lasers up to  $350 \text{ K}$ ', *Electron. Lett.*, 2005, **41**, p. 1175
- 8 Hofstetter, D., Beck, M., Aellen, T., Faist, J., Oesterle, U., Ilegems, M., Gini, E., and Melchior, H.: 'Continuous wave operation of a  $9.3 \mu\text{m}$  quantum cascade laser on a Peltier cooler', *Appl. Phys. Lett.*, 2001, **78**, p. 1964
- 9 Choa, F., Cheng, L., Ji, X., Liu, Z., Wasserman, D., Howard, S.S., Gmachl, C.F., Wang, X., Fan, J., and Khurgin, J.: 'MOCVD growth and regrowth of quantum cascade lasers', *Proc. SPIE*, 2007, **6485**, p. 64850
- 10 Tsekoun, A., Go, R., Pushkarsky, M.B., Razeghi, M., and Patel, C.K.N.: 'Improved performance of quantum cascade lasers through a scalable manufacturable epitaxial-side-down mounting process', *Proc. Nat. Acad. Sci.*, 2006, **103**, pp. 4831–4835